

PIV AND OH LIF IMAGING OF FLAME- VORTEX INTERACTIONS IN AN OPPOSED- JET BURNER

James R. Gord,¹ Jeffrey M. Donbar,¹ Gregory J. Fiechtner,² Campbell D. Carter,² and J. C. Rolon³

- ¹Propulsion Directorate, Air Force Research Laboratory, Wright-Patterson Air Force Base, OH 45433-7103, USA.
- ²Innovative Scientific Solutions, Inc., 2786 Indian Ripple Road, Dayton, OH 45440-3638, USA.
- ³Laboratoire d'Énergétique Moléculaire et Macroscopique, Combustion, École Centrale Paris, Grande Voie des Vignes, 92295 Châtenay-Malabry Cedex, France.

Ninth International Symposium on Applications
of Laser Techniques to Fluid Mechanics

July 13-16, 1998
Lisbon, Portugal

PIV AND OH LIF IMAGING OF FLAME-VORTEX INTERACTIONS IN AN OPPOSED-JET BURNER

James R. Gord,¹ Jeffrey M. Donbar,¹ Gregory J. Fiechtner,² Campbell D. Carter,² and J. C. Rolon³

¹Propulsion Directorate, Air Force Research Laboratory, Wright-Patterson Air Force Base, OH 45433-7103, USA.

²Innovative Scientific Solutions, Inc., 2786 Indian Ripple Road, Dayton, OH 45440-3638, USA.

³Laboratoire d'Énergétique Moléculaire et Macroscopique, Combustion, École Centrale Paris, Grande Voie des Vignes, 92295 Châtenay-Malabry Cedex, France.

ABSTRACT

The dynamic interaction between a laminar flame and a vortex is examined. The hydroxyl (OH) layer produced by the flame is imaged using planar laser-induced fluorescence (PLIF), and preliminary vortex-characterization data are acquired using acetone PLIF and digital, two-color particle-image velocimetry (PIV). The hydrogen-air flame is supported in a nonpremixed opposed-jet burner. The apparatus is found to produce highly repeatable events, making it ideal for studying the interaction between a flame and an isolated vortex. A distinct annular extinction of the OH layer is observed, in good agreement with previous computational modeling predictions of the apparatus. In cases with no extinction of the OH layer, enhanced burning is observed during the flame-vortex interaction.

1. INTRODUCTION

Recent results in numerical modeling combined with experimental measurements have led to important advances in the understanding of combustion. Numerous investigations have contributed to these advances, including a particular type of study in which the interaction between a laminar nonpremixed flame and a vortex is examined. These experiments involve repeatable, carefully controlled conditions that are highly amenable to experimental study.

In recent computational calculations, Katta (1998) predicted that, during the interaction of a nonpremixed hydrogen-air flame and an isolated vortex, the extinction of the OH layer would occur in an annular pattern. The experiments detailed in this paper are carried out to examine, in part, the validity of this prediction. Experimental results obtained with planar laser-induced fluorescence (PLIF) of OH are used to determine regimes in which the annular, Katta-type extinction occurs. The nonpremixed flame is supported by air and fuel in an opposed-jet burner. The fuel consists of hydrogen diluted with nitrogen. The amount of

hydrogen in nitrogen is varied, along with the strength of the vortex. The temporal evolution of flame-vortex interactions is imaged with the PLIF system.

Recently, additional measurements have been initiated for characterization of vortices. First, acetone is seeded into the vortex and its laser-excited fluorescence is detected. Second, particles are seeded into the flowfield, and the scattering is used for digital, two-color particle-image velocimetry (PIV) measurements. Preliminary results from the use of both techniques are discussed in this paper.

2. BACKGROUND

Numerous experimental studies of the interaction dynamics of vortices and flames have been conducted, and many of these investigations employed two-dimensional imaging to study the interaction. For premixed flame fronts, most measurements have been made using two types of flames. Hertzberg et al. (1984) and Escudie (1988) conducted an experiment in which a Karman vortex street was produced using a cylindrical rod in a cross flow of premixed gases. A V-flame was supported behind a wire positioned downstream of the rod that produced the vortex street. Planar tomographic imaging was used to study the interaction of the vortex street with the flame. A similar interaction between a Karman vortex street and a flame was investigated by Lee et al. (1993) using PLIF imaging of OH and by Nye et al. (1996) using both OH PLIF and PIV. A disadvantage of the vortex street is the difficulty in isolating a single vortex. Nguyen and Paul (1996) studied a more isolated interaction by replacing the Karman vortex street with a vortex that was directed into one side of a V-flame. The vortex-injection process was found to be highly repeatable.

In a second type of study involving premixed combustion, Jarosinski et al. (1988) studied a flame that was ignited at one end of a tube of premixed gases. A vortex was injected at the other end of the tube. The

interaction dynamics were then photographed using a mercury-xenon arc lamp and a rotating-drum streak camera with a rotating-disc shutter. Recently, Driscoll et al. (1994) produced an impressive series of papers concerning a similar flame-vortex apparatus in which either PIV or OH PLIF (or a combination of these imaging techniques) was applied.

Nonpremixed flames have also been the subject of experimental investigation. Rolon et al. (1995) recently developed an apparatus in which a vortex is injected into a flame supported between the nozzles of an opposed-jet burner. This geometry has numerous advantages. First, a stationary flame can easily be produced and isolated. Second, the flame thickness can be varied by changing either the nozzle velocities or the spacing between the upper and lower burner nozzles. More recently, Chen and Dahm (1997) developed a facility for generating a non-premixed burning layer that wraps into a vortex ring. The resulting combustion is studied under conditions of normal gravity and microgravity.

The experiments described in this paper are based on the counterflow geometry of Rolon et al. (1995), and the observations described below rely heavily on the progress outlined in their papers. A fuel mixture of hydrogen and nitrogen allows the use of laser diagnostics in the absence of hydrocarbon interferences, and the reaction zone of these nonpremixed flames is generally much thicker than that for premixed flames. The comparatively simple hydrogen-chemistry mechanisms simplify numerical calculations that are the subject of comparison with experimental results.

3. APPARATUS AND PROCEDURE

3.1 Burner Facility

A picture (a) and diagram (b) of the burner are shown in Figure 1. The configuration is based on the design of Rolon et al. (1995). The flame is supported between upper and lower nozzles separated by 40 mm, each with an exit diameter of 25 mm. The fuel consists of hydrogen diluted with nitrogen and flows from the upper nozzle. Air flows from the lower nozzle. Unique to this type of apparatus is a tube with 5-mm inner diameter that is installed concentrically within the lower nozzle. This tube is attached to a cylinder that contains a piston, which is, in turn, attached to an actuator. Feeding an appropriate current to the actuator causes a solenoid to force the piston upward abruptly, resulting in the emergence of a vortex from the tube. The vortex travels upward within the surrounding oxidizer flow. A flow of air is supplied to the vortex tube such that, in the absence of a vortex, the exit velocity matches the velocity of the surrounding nozzle. To minimize the

impact of room-air disturbances, upper and lower guard flows of nitrogen are supported through outer nozzles.

The hydrogen, nitrogen diluent, and oxidizer air flows are provided by mass-flow controllers with full-scale ranges of 20 l/min, 20 l/min, and 30 l/min, respectively. A continuous flow of air is provided to the vortex tube by a 5-l/min controller, while the guard flow from the upper and lower guard nozzles is provided by two 50-l/min mass flow controllers. The flow rates of each controller are good to $\pm 1\%$ of the full-scale range. The experiments have been repeated for several different flame conditions, as summarized in Table I.

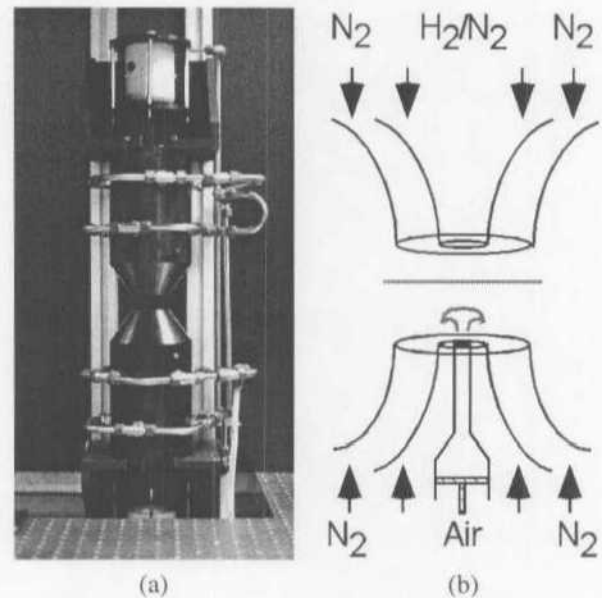


Figure 1. (a) Digital photograph of the opposed-jet burner. (b) Cross-sectional diagram of the burner nozzles and piston.

Table I. Flow rates (l/min) at 21.5°C and 724 mm Hg for five flame conditions. X_{H_2} is the volume fraction of hydrogen in nitrogen diluent.

Gas	Flame					
	A	B	C	D	E	F
H ₂	2.76	3.40	4.04	4.67	5.31	5.94
N ₂ Diluent	17.1	17.1	17.1	17.0	17.0	16.9
X_{H_2}	0.14	0.17	0.19	0.22	0.24	0.26
Air	11.2	11.2	11.2	11.2	11.2	11.2

The vortex properties can be varied by changing the magnitude and the rise time of the current that is fed to the actuator. The impedance of the actuator is in the range from 1 Ω to 1.5 Ω , depending on the frequency content of the current. At full displacement, a current of up to 6 A is provided to the solenoid by a specially

designed, high-speed power amplifier. This can result in considerable power consumption by the actuator if the full displacement condition is maintained for long periods of time. Consequently, an AC waveform is supplied by the initial application of a negative potential, causing the piston to be withdrawn away from the flame. The negative potential is applied for about 0.5 s to allow the flame to recover from this initial disturbance, which is verified by digital, two-color PIV. The potential is then quickly changed to a positive value of the same magnitude with a precisely controlled rise time, τ_r . The strength of the vortex can be increased by increasing the current magnitude, which results in a larger displaced fluid volume through the exit of the tube. Eventually, the maximum displacement of the solenoid is reached. In this case, the vortex strength can also be increased using a smaller value of τ_r . The relationship among volume displacement, τ_r , and the vortex characteristics has been discussed in numerous papers, including those by Rolon et al. (1995), Roberts (1992), and Chen and Dahm (1997). The drive current for the solenoid is obtained by power amplifying the output of a digital arbitrary-waveform generator. This generator is operated at its maximum number of 10 000 quantized steps, resulting in a minimum stepsize of 0.1 ms. For all measurements discussed in this paper, τ_r is set at 10 ms.

Visualization of the vortex formation and propagation via acetone PLIF is accomplished using a vaporizer that is installed between the vortex tube and the mass-flow controller. A bypass valve allows the choice of acetone seeding level. Because the acetone changes the flame characteristics, these visualization studies are limited to non-reacting flows. When the acetone studies are not required, the acetone vaporizer is removed from the apparatus.

Seed particles are introduced into the burner flows when digital PIV measurements of the velocity of the vortex are performed. Three particle seeders are installed: One seeder is placed after the oxidizer-air mass-flow controller and another after the vortex-air mass-flow controller. The third seeder is installed after the junction where the hydrogen and nitrogen gases are mixed. With the use of three seeders, each flow can be seeded with particles individually, or combinations of the different flow fields can be seeded. Each seeder contains hollow spherical ceramic particles with an approximate mean diameter of 2.4 μm . When PIV studies are not required, the seeders are removed from the apparatus.

3.2 Laser Diagnostics

The PLIF system contains a frequency doubled, Q-switched Nd:YAG laser that is used to pump a fre-

quency-doubled dye laser. The light is directed through a telescope that is adjusted to produce a light sheet with a height that matches as nearly as possible the 40-mm burner separation. The resulting beam thickness is $\sim 300 \mu\text{m}$, which corresponds to the full width at 25% of the peak of the intensity profile, and $\sim 15 \text{ mJ/pulse}$ is available at the test section.

Hydroxyl radicals absorb the laser radiation at 281.3414 nm via the $R_1(8)$ transition of the (1,0) band in the A-X system. Fluorescence from the A-X (1,1) and (0,0) bands is detected at right angles through WG-295 and UG-11 colored-glass filters, followed by a 105-mm focal length, f/4.5 UV lens. The resulting light reaches an intensified CCD camera with an intensifier gate width of 100 ns. CCD pixels are binned in groups of 2×2 . Data are stored on a personal computer. A color table is used with a maximum value set to 95% of the maximum signal for all images taken at a given flame condition. The low-signal color is assigned by calculating the background noise and selecting a minimum value that is two standard deviations above this level. Therefore, in cases where "extinction" of the OH layer is observed, "extinction" refers to signal levels that fall below this minimum value and are, therefore, assigned the last color in the table. All images represent the signal collected during a single laser shot, and no smoothing of the resulting images is attempted.

In studies of flame-vortex interactions by Najm et al. (1998), LIF was applied as a marker of some other quantity such as heat release or burning rate. In the present experiments, the OH image is obtained for direct comparison with numerical computations of the OH distribution; therefore, no attempt is made to correlate the images with any other quantities.

Acetone PLIF imaging is accomplished using the OH PLIF imaging system. Here, the UG-11 colored-glass filter is removed to permit collection of the acetone fluorescence.

Recent measurements of the velocity field have been implemented using digital, two-color PIV. Here, the ICCD camera is replaced with a color digital CCD. This type of CCD has a mask with green-transmissive filters for 50% of the pixels, red-transmissive filters for 25% of the pixels, and blue-transmissive filters for the remaining 25% of the pixels. Two lasers are used, with one sheet being produced by directly doubling the output of a Q-switched Nd:YAG laser (30 mJ/pulse at the test section). The second light sheet is produced by pumping a dye laser (employing DCM laser dye) with a second frequency-doubled, Q-switched Nd:YAG laser, resulting in laser radiation at 640 nm (40 mJ/pulse at the test section). The thickness of both the red and green sheets is set to $\sim 700 \mu\text{m}$. A digital delay generator is used to drive the timing of the two lasers such that the

red pulses are delayed by a precisely controlled amount of time with respect to the green pulses. In the absence of a vortex, the underlying counterflow velocity field is probed with red pulses that are delayed by up to 1 ms with respect to the corresponding green pulses. For the fastest vortices studied, the delay between red and green pulses is reduced to 10 μ s. The camera shutter is set to be open for 1/15 s to permit both laser pulses to be detected by the color CCD. Most of the flame emission and light emitted by other devices (monitors, etc.) in the laboratory is greatly attenuated by the shutter. Velocity vectors are calculated using the correlation software of Gogenini et al. (1998).

3.3 Synchronization and Timing

Precise synchronization of several experimental events, including vortex generation and propagation, production of laser pulses, and activation of the camera shutter or intensifier, is required. A block diagram of the synchronization scheme is shown in Figure 2.

Because the Nd:YAG lasers are designed to operate at a nominal repetition rate of 10 Hz, the experimental sequence must be synchronized to a 10-Hz master clock that drives the flash lamps and the Pockels cells of the lasers. To trigger the laser(s), the clock sends two signals, one of which travels to a 50- Ω power combiner and then the laser digital delay generator

(DDG). The 10-Hz clock also provides a TTL signal to one of two inputs of a coincidence unit. The second input of the coincidence unit is driven by a TTL pulse from the PLIF camera controller. The coincidence unit outputs a pulse only when pulses from both the 10-Hz clock and the PLIF camera controller are present. When a flame-vortex event is initiated using a personal computer, the PLIF camera controller outputs a pulse \sim 1.3 s in duration. The corresponding output of the coincidence unit is a 1.3-s envelope of TTL pulses spaced by 100 ms. The first pulse in this envelope triggers a master DDG, synchronizing it with the 10-Hz clock and the laser pulse train. This DDG triggers an arbitrary-waveform generator (AWG) that outputs a 1-s waveform, which is amplified and fed to the piston actuator to generate a vortex. Approximately 0.5 s after the AWG waveform is initiated, the vortex is fired; therefore, five laser pulses are generated during the time between computer initiation and the flame-vortex interaction.

When the DDG is externally triggered, the jitter between the trigger and a DDG output pulse is 60 ps plus the output delay divided by 10^8 . Over the 0.5-s period between the first and fifth laser pulses, this corresponds to a jitter of 5.06 ns. The DDG clock jitter specifications are not nearly so good. The jitter between clock outputs is 1 part in 10 000, corresponding to a

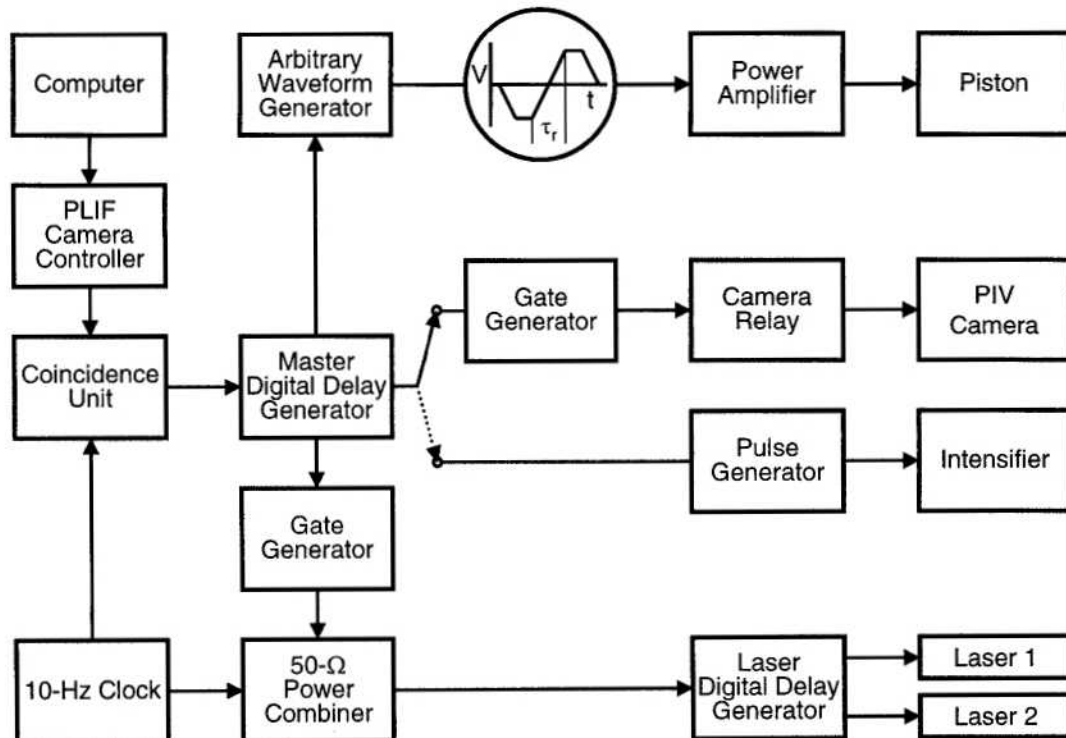


Figure 2. Diagram of electronic timing connections.

jitter of $50\ \mu\text{s}$ over the same 0.5-s period. Attempting to synchronize the piston with the clock severely limits the temporal resolution available to “freeze” flame-vortex events in time and requires an intensifier gate width significantly larger than $50\ \mu\text{s}$. The master DDG is therefore configured to trigger the fifth laser pulse preemptively. A delayed pulse from the master DDG arrives at the $50\text{-}\Omega$ power combiner just before the fifth pulse in the clock pulse train, preemptively triggering the laser(s). If no initiation pulse is output from the computer, the laser(s) are triggered by the 10-Hz clock as usual. This approach reduces the jitter in the timing of the fifth laser pulse from $50\ \mu\text{s}$ to $\sim 5\ \text{ns}$ while maintaining the nominal 10-Hz repetition rate required by the lasers.

Another output of the master DDG is suitably delayed and directed to the image detector. For PIV experiments, the width of this TTL pulse is adjusted using a gate generator, which closes a relay to trigger the digital PIV camera system. For PLIF experiments, this master DDG output triggers a pulse generator, which, in turn, activates the intensifier of an ICCD camera.

The scheme depicted in Figure 2 provides precise control of the relative timing between the laser diagnostics and the flame-vortex event. To explore the temporal evolution of the event, data are captured utilizing this phase-locked timing sequence: 1) an image is recorded, 2) the delay between vortex production and the laser/camera events is adjusted, and 3) another vortex is initiated and a second image is recorded. This process is repeated to acquire numerous images, each obtained at increasing delay. An animation is then created by assembling the individual images in temporal order. Effective temporal separation between images is selected between $10\ \mu\text{s}$ and $200\ \mu\text{s}$, depending on the time scale of the event under study. The resulting animations are a testament to the high degree of repeatability achievable with this apparatus.

4. RESULTS AND DISCUSSION

4.1 Vortex Characterization

The sequence of acetone images in Figure 3 is typical of the sequential images used to measure the vortex-propagation velocity for a given amplitude and rise time of the solenoid drive current. The six images in the figure are selections from a sequence of 50 images, each delayed by $100\ \mu\text{s}$ relative to the previous image. If the location of the flame front in the absence of a vortex is known, the acetone PLIF image sequence can be used to estimate the velocity of the vortex at this location. In this case, the propagation velocity is $\sim 5\ \text{m/s}$.

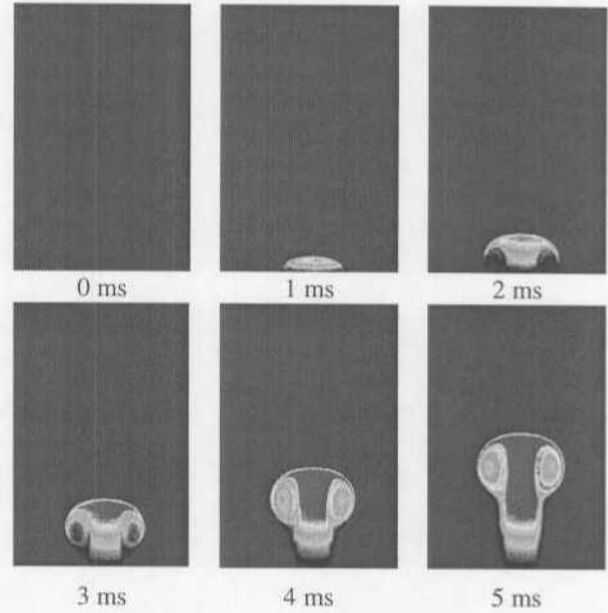


Figure 3. Acetone PLIF images of vortex.

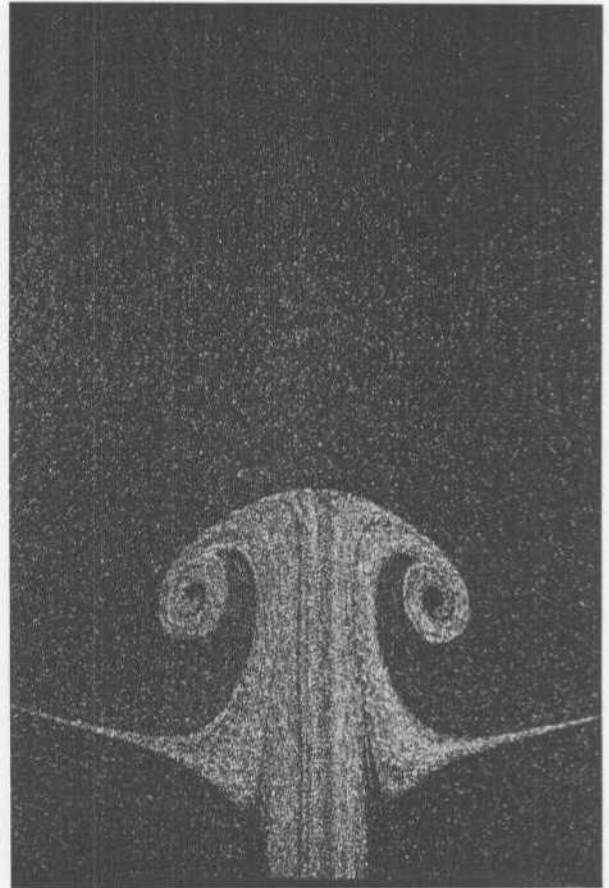


Figure 4. Scattering from particles in vortex flow.

Recently, characterization of vortex properties has been initiated using PIV. For example, Figure 4 contains the scattering signal obtained when seeding the vortex tube flow with a slightly higher particle density than that produced by the upper and lower burner seed levels. The corresponding set of vectors is shown in Figure 5. The maximum vector length in the forward direction yields a propagation velocity of 0.77 m/s. Digital, two-color PIV measurements are readily made when the flame is burning, offering a significant advantage over the acetone PLIF measurements of the vortex-propagation velocity.

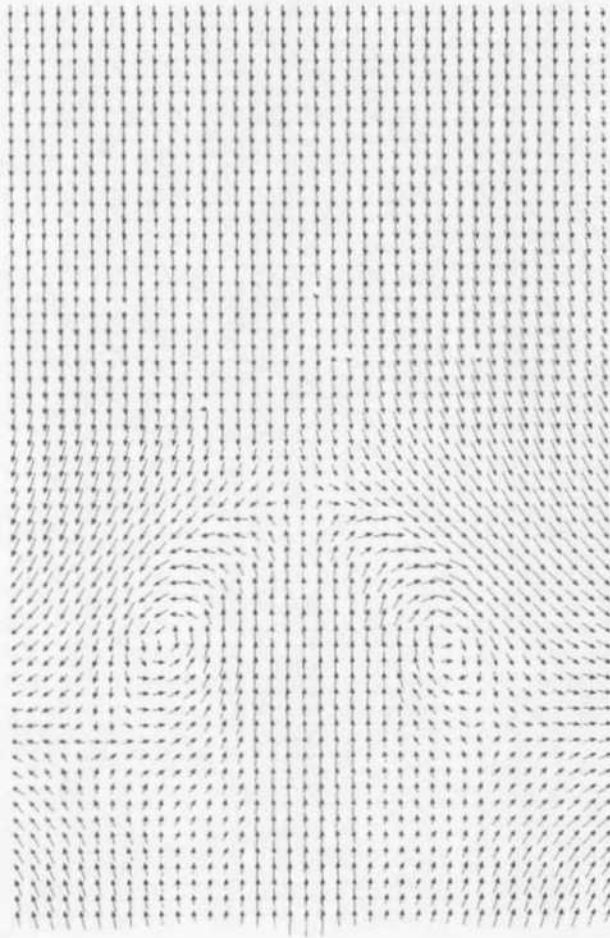


Figure 5. Vectors calculated using the PIV image of Figure 4.

4.2 Regimes of Flame-Vortex Interaction

The PLIF images of OH shown in Figure 6 correspond to a flame-vortex interaction in which extinction of the OH layer is absent. Initially, the vortex creates a small dent in the flame, and this dent then grows. Eventually the flame nearly surrounds the advancing vortex as it approaches the upper nozzle. In the later

interaction stages, the OH PLIF signal level is observed to increase by up to a factor of five over the levels observed without a vortex. The increased signal level is

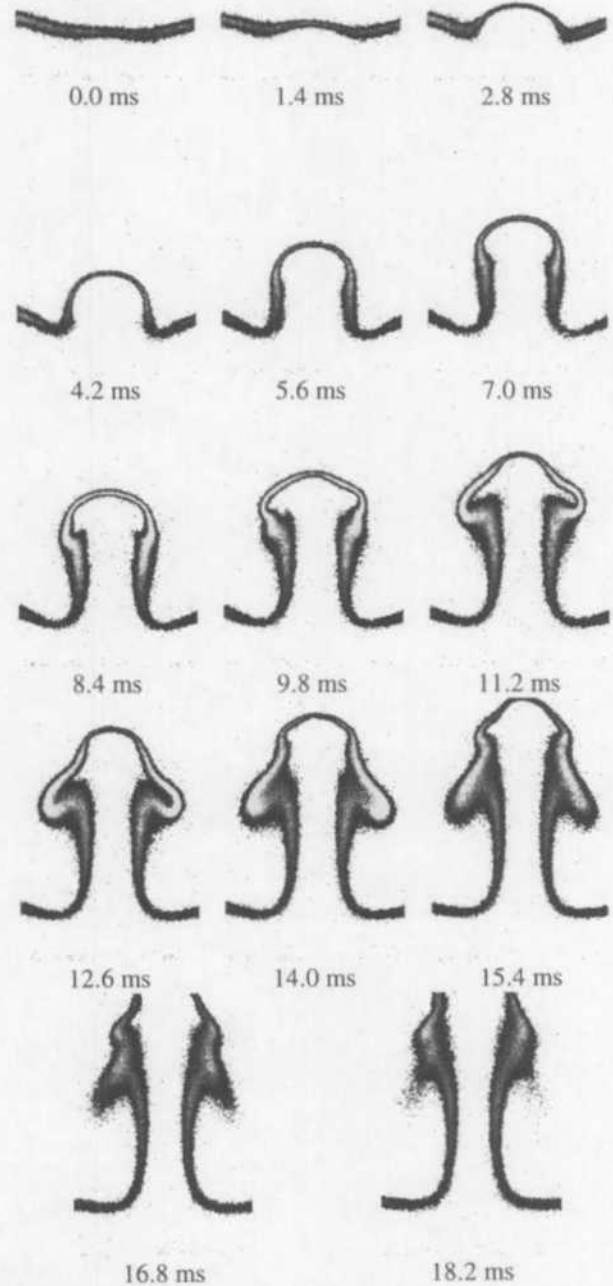


Figure 6. OH PLIF images when OH layer remains intact.

indicated by the light regions of the OH layer in the frames of Figure 6. This change in OH signal level is thought to indicate enhanced burning. For this particular example, the flow rates of Flame D of Table I are

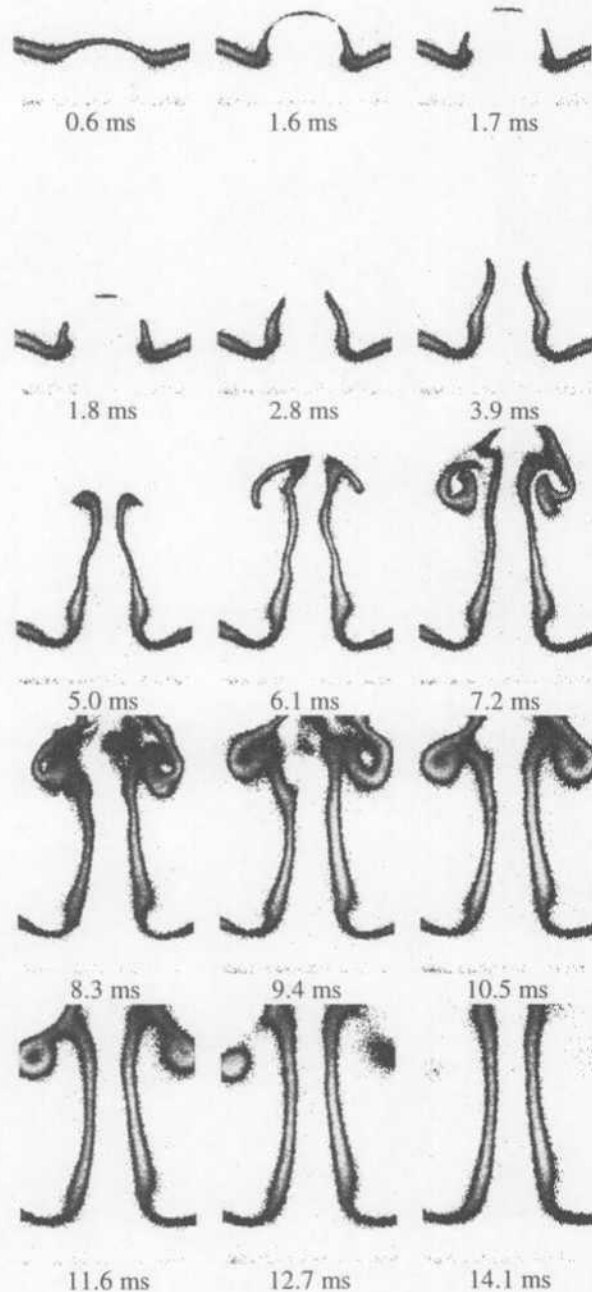


Figure 7. Sequence of images before and after extinction of the OH layer.

used. The images of Figure 7 are obtained with flow conditions corresponding to Flame E of Table I. Extinction of the OH layer takes place in an annular pattern around the sides of the vortex, leaving a burning layer at its leading edge. This behavior was first predicted numerically by Katta [1], well before these experiments were initiated, attesting to the utility of his code. After extinction, the isolated island of flame burns away, and the vortex travels upward toward the other nozzle. The flame follows the vortex, traveling up the stem. As the flame overtakes the vortex, it wraps up and turns in on itself.

To test the temporal resolution of the instrument, a series of sequential images was taken with a delay of 10 μ s. The region of study consisted of frames about 1.8-ms delay shown in Figure 7. This delay regime was chosen to focus on the so-called Katta effect. The repeatability of the apparatus of Rolon et al. (1995) is observed to be exceptional.

5. CONCLUSIONS AND FUTURE RESEARCH

The apparatus of Rolon et al. (1995) has been implemented for the study of the interaction of a flame with a vortex. PLIF measurements of acetone and digital, two-color PIV have been applied to characterize the vortices injected into the opposed-jet flow. PLIF images of OH have been used to observe the dynamics of the interaction of the flame with the vortex. These combined measurements show that this burner can provide effective temporal resolution to at least the 10- μ s level. An annular break in the OH layer has been observed, in excellent agreement with the numerical computations of Katta (1998).

Future work will be directed toward understanding phenomena such as the Katta-type extinction. A variety of parameters can be studied, such as extended ranges of nitrogen dilution in hydrogen, different flame-thickness regimes, and different fuels. To aid in these studies, simultaneous OH PLIF and digital, two-color PIV are presently being implemented, along with measurements of the temperature field.

ACKNOWLEDGEMENTS

The authors are grateful to Mr. K. D. Grinstead, Jr., for assistance in synchronization of the experiment and construction of the solenoid power amplifier. In addition, the authors wish to acknowledge the advice of Dr. L. P. Goss concerning the reduction of two-color PIV data. The authors wish to thank Dr. R. D. Hancock for assistance in assembly and construction of the burner. The authors also acknowledge Drs. R. D. Hancock, W. M. Roquemore, V. R. Katta, and K.-Y.

Hsu for the stimulating discussions of flame-vortex dynamics. Finally, the authors wish to thank M. M. Whitaker for editing this manuscript. This work was supported by Air Force Contracts F33615-95-C-2507 and F33615-97-C-2702.

REFERENCES

- Chen, S.-J. & Dahm, W. J. A. 1997, Vortex Ring/Diffusion Flame Interactions in Microgravity Conditions, Fourth International Microgravity Combustion Workshop, Cleveland, OH, pp. 191-196. NASA Conference Publication No. 10191.
- Driscoll, J. F., Sutkus, D. J., Roberts, W. L., Post, M. E., & Goss, L. P. 1994, The Strain Exerted by a Vortex on a Flame—Determined from Velocity Field Images, Combust. Sci. Technol., Vol. 96, No. 4/6, pp. 213-229. See also: Roberts, W. L., & Driscoll, J. F. 1991, A Laminar Vortex Interacting with a Premixed Flame: Measured Formation of Pockets of Reactants, Combust. Flame, Vol. 87, No. 3/4, pp. 245-256; Roberts, W. L., Driscoll, J. F., Drake, M. C., & Ratcliffe, J. W. 1992, OH Fluorescence Images of the Quenching of a Premixed Flame During an Interaction with a Vortex, Twenty-Fourth Symposium (International) on Combustion, The Combustion Institute, Pittsburgh, PA, pp. 169-176; Roberts, W. L., Driscoll, J. F., Drake, M. C., & Goss, L. P. 1993, Images of the Quenching of a Flame by a Vortex—To Quantify Regimes of Turbulent Combustion, Combust. Flame, Vol. 94, No. 1/2, pp. 58-69; Mueller, C. J., Driscoll, J. F., Ruess, D. L., & Drake, M. C. 1996, Effects of Unsteady Stretch on the Strength of a Freely-Propagating Flame Wrinkled by a Vortex, Twenty-Sixth Symposium (International) on Combustion, The Combustion Institute, Pittsburgh, PA, pp. 347-355; Mueller, C. J., Driscoll, J. F., Ruess, D. L., Drake, M. C., & Rosalik, M. E. 1998, Vorticity Generation and Attenuation as Vortices Convect Through a Premixed Flame, Combust. Flame, Vol. 112, No. 3, pp. 342-358.
- Escudie, D. 1988, Stability of a Premixed Laminar V-Shaped Flame, Prog. Astronaut. Aeronaut., Vol. 113, pp. 215-239.
- Gogineni, S., Goss, L., Pestian, D., & Rivir, R. 1998, Two-Color Digital PIV Employing a Single CCD Camera, Exp. Fluids, in press.
- Hertzberg, J. R., Namazian, M., & Talbot, L. 1984, A Laser Tomographic Study of a Laminar Flame in a Karman Vortex Street, Combust. Sci. Technol., Vol. 38, No. 3/4, pp. 205-216.
- Jarosinski, J., Lee, J. H. S., & Knystautas, R. 1988, Interaction of a Vortex Ring and a Laminar Flame, Twenty-Second Symposium (International) on Combustion, Pittsburgh, PA, pp. 505-514.
- Katta, V. R., Carter, C. D., Fiechtner, G. J., Roquemore, W. M., Gord, J. R., & Rolon, J. C. 1998, Interaction of a Vortex With a Flat Flame Formed Between Opposing Jets of Hydrogen and Air, accepted for publication in Twenty-Seventh Symposium (International) on Combustion The Combustion Institute, Pittsburgh, PA.
- Lee, T.-W., Lee, J. G., Nye, D. A., & Santavicca, D. A. 1993, Local Response and Surface Properties of Premixed Flames During Interactions with Karman Vortex Streets, Combust. Flame, Vol. 94, No. 1/2, pp. 146-160.
- Najm, H. N., Paul, P. H., Mueller, C. J., & Wyckoff, P. S. 1998, On the Adequacy of Certain Experimental Observables as Measurements of Flame Burning Rate, Combust. Flame, Vol. 113, No. 3, pp. 312-332.
- Nguyen, Q.-V. & Paul, P. H. 1996, The Time Evolution of a Flame-Vortex Interaction Observed via Planar Imaging of CH and OH, Twenty-Sixth Symposium (International) on Combustion, The Combustion Institute, Pittsburgh, PA, pp. 357-364.
- Nye, D. A., Lee, J. G., Lee, T.-W., & Santavicca, D. A. 1996, Flame Stretch Measurements During the Interaction of Premixed Flames and Karman Vortex Streets Using PIV, Combust. Flame, Vol. 94, No. 1/2, pp. 167-176.
- Roberts, W. L. 1992, A Premixed Laminar Flame Interacting With a Vortex Resulting in Flame Stretch and Quenching, Ph.D. Dissertation, University of Michigan, Ann Arbor, MI.
- Rolon, J. C., Aguerre, F., & Candel, S. 1995, Experiments on the Interaction Between a Vortex and a Strained Diffusion Flame, Combust. Flame, Vol. 100, No. 3, pp. 422-429. See also: Thevenin, D., Rolon, J. C., Renard, P. H., Kendrick, D. W., Veynante, D., & Candel, S. 1996, Structure of a Non-Premixed Flame Interacting with Counterrotating Vortices, Twent-Sixth Symposium (International) on Combustion, The Combustion Institute, Pittsburgh, PA, pp. 1079-1086.